

# Review of Accomplishments in Abrasive-Waterjet from Macro to Micro Machining -Part 1

H.T. Peter Liu<sup>1</sup>

<sup>1</sup> OMAX Corporation

*Received: 16 December 2019 Accepted: 31 December 2019 Published: 15 January 2020*

---

## Abstract

Abrasive-waterjet (AWJ) technology possesses inherent characteristics unmatched by most machine tools. The initial commercialization of AWJ in the mid1980s was to take advantage of its superior cutting power for raw cutting of thick and difficult-to-machine materials. Subsequently, considerable RD was devoted to take full advantage of the above characteristics while refining machining processes toward precision machining and automation. This two-part paper presents the accomplishments that advance AWJ technology in terms of improving the cutting accuracy and efficiency, broadening applications for machining delicate materials from macro to micro scales, and enabling 3D capability for multimode machining. In Part 1 of the paper, six topical areas are presented to demonstrate some of the important achievements in advancing AWJ technology. The areas include: - control software, meso-micro and stack machining, macro to micro machining, cold cutting, hole drilling, and gear making. Additional topical areas will be presented in Part 2 of the paper to fully explore the technological and manufacturing merits of AWJ technology. Such merits had elevated AWJ technology as one of the most versatile machine tools competing on equal footing, and with advantage in some cases, among subtractive and additive manufacturing tools. The accomplishments presented in this paper had clearly demonstrated that AWJ technology was capable of multi-mode machining for most materials from macro to micro scales, the ?7M? advantage. The versatility of AWJ technology has clearly demonstrated its ?7M? advantage.

---

*Index terms—*

## 1 Introduction

n 1973, after joining Flow Research, Inc., where the waterjet technology was developed and commercialized, the author had the privilege of participating in R&D activities to advance the technology. 1 He subsequently joined OMAX Corporation in 2005 and continued his pursue in advancing waterjet technology. He was involved in the commercialization of the technology while witnessing its maturing and growth in the adaptation by the manufacturing community. In the early stage, when the abrasive waterjet (AWJ) was commercialized in the mid1980s, a reasonable controller to maneuver the operation had yet to be developed. It merely served as a raw cutting tool for difficult-to-cut I and thick materials to take advantage of its superior cutting power. As the technology advanced, additional technological and manufacturing merits were discovered and progressively verified. Among the merits in addition to the superior cutting power are green machining process, material independence, cold cutting, adaptability to automation, amenability to micromachining, low loading on work pieces, and 3D capability (Liu and Schubert, 2012;Liu, 2017a). Most of the development efforts in the last three decades, in addition to hardware improvement for cutting performance, were to develop controller and smart software for operating the machine toward precision machining. In modern times, AWJ possesses technological

and manufacturing merits that are superior to most other tools. It has been elevated as a modern machine tool competing on equal footing among lasers, electrical discharged machining (EDM), and precision milling tools.

Since AWJ carries out machining by means of a high-speed and thin beam of water-only-jet (WJ) and AWJ, it is amenable to micromachining. Recent success in commercialization of micro abrasive-waterjet ( $\mu$ AWJ) technology has broadened the range from macro to micro machining. The diameter of the WJ was defined by the diameter of the orifice, the single phase WJ with diameters smaller than 100  $\mu$ m has been used to cut relatively soft materials such as fabrics, rubber, foam, thin plastics, and various food products (Yadav and Singh, 2016). With the entrainment of abrasives and air together with the incorporation of the mixing tube, the diameter of the three-phase AWJ is about three to four times that of the WJ. At present, the smallest kerf width achievable with commercially available AWJ systems is around 300 to 400  $\mu$ m. Preliminary tests using a research  $\mu$ AWJ nozzle, with a 76  $\mu$ m orifice and a 175  $\mu$ m mixing tube, showed that a kerf width of 200  $\mu$ m was achievable (Liu and Gershenfeld, 2020). Very thin materials that are too delicate to machine otherwise can be machined by stacking multiple layers of materials with the powerful AWJ. The increase in the thickness of the stack not only stiffens the individual layers for ease of fixturing but also allows utilization of the Tilt-A-Jet for machining nearly taper free edges of individual thin materials within the stack. 2 AWJ is capable of machining most materials from metal, nonmetal, to anything in between, whether they are conductive or nonconductive and reflective or non reflective. In particular, AWJ will meet the challenge of machining nanomaterials integrated with various material types possessing nonlinear material properties (Liu, 2017b). Such nanomaterials would present considerable challenge to conventional tools. As a cold cutting tool without the introduction of a heat-affected zone (HAZ), AWJ often is capable of cutting one order of magnitude faster than solid state lasers (pulsed at high frequency) and wire EDM (cut with multiple passes) (Liu, 2019a). For extremely high precision parts made of difficult-to-cut materials, end mills and spindles are often subject to severe tool wear resulting in high retooling costs. AWJ could preferably apply as a near-net shaping tool to remove the bulk of the materials. Near-net shaped parts can then be finished via light trimming with precision CNC tools. Such a hybrid process, particularly for delicate and difficult-to-machine materials, would speed up the turnaround time while minimizing the retooling costs.

The unconventional AWJ differs from most machine tools as its cutting tool is a flexible beam of abrasive slurry. One of the emphases to achieve superior precision is to develop smart control software to mitigate anomalies induced by the flexibility of the AWJ. Continued advancements in AWJ technology would unleash its potential to be one of the all-in-one and one-in-all process to machine a wide range of advanced materials that present considerable challenge to most machine tools. The benefits would include the preservation of structural and chemical properties of parent materials, extension of tool lives, and expediting turnaround time leading to significant overall cost saving.

Future advancement in AWJ technology is expected to develop an all-in-one and one-in-all tool for precision machining from macro to micro scales. Continued efforts are underway to improve the cutting accuracy and to further downsize  $\mu$ AWJ nozzles. In this two-part paper, recent advancements in AWJ technology to take advantage of its technological and manufacturing merits are described. In particular, emphasis will be made to present several established and new trends in applying AWJ for precision machining.

## 2 II. R&D and Demonstration Facilities

OMAX is equipped with two laboratories for R&D and demonstration. The R&D Lab is dedicated to engineering research and development from components and processes, cutting model, to nozzle to respond for taper compensation, The lag in the response could lead unacceptable anomalies. These accessories were used in machining the sample parts presented in the paper. A combination of multiple accessories were often used to machine certain features. For example, the combined operations of the A-Jet and Rotary Axis can be used to machine rather complicated 3D features such as the "fish mouth" saddle weld joints on pipes and features on curved surfaces.

There are R&D and manufacturing machine shops equipped with CNC machines for fabricating components used in R&D activities and assembling the four product lines of waterjet systems. Various instruments and devices are available in the laboratories and Quality Control Department for measuring parameters to quantify the part geometries such as edge taper, surface roughness, part accuracy, and others. Several sample parts presented herein were made by academic and industrial collaborators. Their tools will be described briefly where these parts are presented.

## 3 III.

## 4 Advances in awj Technology

### 5 a) Controller software

Based on the fact that AWJ process is adaptable to digital machining, considerable efforts were placed to develop PC-based computer numeric control (CNC) software toward automation. The Intelli-MAX Software Suite was developed to take abrasive waterjet cutting to the industry's highest levels of speed and performance. The Suite contains a collection of a number of PC-based software modules related to AWJ machining. Two of the most used modules are the Layout (CAD) and MAKE (CAM). LAYOUT is used to transform the design

intent into a continuous tool path by adding Lead-In and Lead-Out (the entry and exit of the AWJ stream to cut paths) to different parts of the tool path. LAYOUT uses colors to represent five different performance testing. The Demo Lab is mainly for demonstrating AWJ machining for prospective and existing clients. There are several Jet Machining® Center (JMC) from the four product lines installed in the two laboratories (<https://www.oxam.com/products>). The OMAX 2652 and MicroMAX were used most often for general and meso-micro machining. A number of accessories are installed on these machines to enhance AWJ machining (<https://www.oxam.com/accessories>). Key accessories include but are not limited to:

- ? Tilt-A-Jet (TAJ) for compensating edge.

- ? Rotary Axis (RA) for axisymmetric machining.

- ? A-Jet or articulated jet for beveling and countersinking.
- ? Precision Optical Locator (POL) for facilitating alignment and orientation of pre-machined components for precision machining.
- ? Vacuum Assist (VA) for low-pressure piercing and machining to mitigate nozzle clogging.

3 There are five edge qualities defined for AWJ machining, Q1, Q2, Q3, Q4, and Q5. Q1 and Q5 correspond to the edge qualities of rough and precision cuts, respectively.

edge qualities from rough (Q1) to precision (Q5) cutting. The colors of a LAYOUT drawing indicate the edge quality that will be used to make it. The tool path is saved in an ORD (OMAX Routed Data) file and contains a series of commands for moving the AWJ machining head. The ORD file is then loaded to MAKE to assign cutting parameters based on the cutting model, the brain of the controller software. Since AWJ is not a rigid tool, it must simply be guided along a particular path to make a part with the controller software. In particular, the controller must be designed to correct for several errors induced by the AWJ moving at high speeds, including jet lag, edge striation pattern, edge taper, kerf width, and kickback. For common engineering materials, the cutting model based on the results of extensive cutting tests (Zeng, 2007, Zeng et al., 1992, Liu, 2019b). The value of M is proportional to the cutting speed for a given material. For example, The M indices equal 215, 108, and 81 for aluminum, stainless steel, and titanium, respectively. In other words, waterjet cuts aluminum 215/81 or 2.65 times faster than it cuts stainless steel for the same setup. Since erosion by the impact of high-speed abrasives is the primary mode of material removal, it behaves differently from cutting with CNC hard tools. As such, waterjet cuts titanium 34% faster than it cuts steel.; It also cuts hardened steel nearly as fast as it cuts the annealed counterpart thus saving the need to shape the part in the annealed condition and mitigate the distortion of thermal treatment after shaping. The incorporation of the machinability index into the cutting model enabled waterjet as an automation machining process. In particular, the cutting model has been upgraded through the optimization of cutting processes and strategies to increase the cutting speed without degrading the cutting accuracy. There were three upgrades of the cutting model since it was incorporated into the IntelliMAX Software Suite, each upgrade had led to significant enhancement in the cutting efficiency (Liu et al., 2018a). Figure 1a illustrates three 12.7 mm thick stainless-steel gears cut with three different generation of cutting models. The gears were cut at a quality of Q5 for all three. 3 The lengths of cut for the three gears are 0.28, 0.15, and 0.13 m. The ratio of the lengths of cut, therefore represented the performance of the three cutting models: G4 versus G2 215% and G4 versus G3 187%. Figure 1b shows the cutting times for 10 pieces of identical parts. The ratios of the cutting times are consistent with those of the cutting length. b) Meso-micro and stack machining The diameter of the AWJ is controlled by those of the orifice and mixing tube; it is amenable to micromachining (Miller, 2003;2005). Micro abrasive-waterjet ( $\mu$ AWJ) technology was successfully developed under the support of an NSF SBIR grant (Liu and Schubert, 2012). The  $\mu$ AWJ technology was commercialized in 2013, culminating in a new product -the award-winning MicroMAX® JetMachining® Center. It was equipped with a production 7/15 nozzle with a  $\phi$ 0.007" ( $\phi$  0.18 mm) orifice and  $\phi$ 0.015" ( $\phi$ 0.38 mm) mixing tube is capable of machining features around 0.018" (0.5 mm). 4 A 5/10 nozzle capable of machining features around 0.3 mm has been under beta testing. The  $\mu$ AWJ technology was enhanced through upgrading the MicroMAX by incorporating a Rotary Axis for machining axisymmetric parts and by further downsizing the  $\mu$ AWJ nozzle toward micromachining. Subsequently, experimental nozzles as small as a 2/6 nozzle combination was investigated with good promise.

In parallel to downsizing of the  $\mu$ AWJ nozzle, the size of the garnet abrasives must be reduced accordingly. As a rule of thumb, the average size of the abrasives should be smaller than 1/3 of the internal diameter (ID) of the mixing tube in order to mitigate clogging the mixing tube due to the bridging of two large particles. For the 5/10 and 4/8 nozzles, 240 mesh garnet with an average particle size of 60  $\mu$ m meets the above criterion as the ID of the 4/8 nozzle is 203  $\mu$ m. For the 3/6 nozzle with the ID of the mixing tube equal to 152  $\mu$ m, the 240-mesh garnet no longer meets the above criterion. The next smaller size 320 mesh garnet with an average particle size of 30  $\mu$ m was used instead. Unfortunately, the powdery 320 garnet ceases to flow consistently under gravity feed, as the flow ability of abrasive is known to deteriorate with the reduction in particle size (Xu et al., 2018). One of the common problems is that the flow of fine abrasive is interrupted with the development of "worm hole" inside the hopper. A solution to overcome the poor flow ability of fine abrasives was through the development of patented novel processes and devices. This allowed the successful operation of the downsized  $\mu$ AWJ nozzles. However, it is capable of machining certain features with size near 100  $\mu$ m to take advantage of the cold cutting and low exertion of side force on the work piece (Liu and Gershenfeld, 2020). Figure 2 shows a set of tweezers machined with several nozzles to demonstrate the progress in the development of  $\mu$ AWJ technology toward micromachining.

With the 5/10 nozzle, the kerf width is  $\phi$  300 $\mu$ m. When stacking together with taper compensation using the

TAJ was adopted for the  $\mu$ AWJ, the above advantages of the Zund over the  $\mu$ AWJ disappeared or the trend even reversed. The combined stack machining and taper compensation not only improved the part accuracy and edge quality but also enhanced the productivity of the  $\mu$ AWJ. Comparing to single-sheet machining, AWJ stack cutting cut the aluminum flexure above three times faster than the Zund did. As  $\mu$ AWJ is further downsized toward micromachining of very thin and delicate materials, stack machining would serve as an enhancer to fixture such materials. In collaborating with JPL/NASA, cutting tests were conducted using the  $\mu$ AWJ nozzles to machine several miniature flexures used in prototype microsplines for asteroid grippers developed under the Asteroid Redirect Mission at NASA (Tate, 2013). Comparison of the performance of the  $\mu$ AWJ and wire EDM conducted at JPL, the cost ratio between waterjet and wire EDM was 1:14, leading to a cost reduction to machining, only very low loading was exerted onto the workpiece. This simplifies fixturing to secure the even relatively thin workpieces. The low side force exerted onto the workpiece together with cold cutting enables AWJ cutting very thin walls with large aspect ratios (length-to-width and length-to-thickness) even on delicate materials such as thin glass without deforming them thermally and mechanically (Liu et al., 2018a).

## 6 Global Journal of Researches in

A MicroCutting Project was initiated at the MIT Center for Bits and Atoms (CBA -www.cba.mit.edu) (Liu and Gershenfeld, 2020). The performances of  $\mu$ AWJ and several subtractive and additive tools were compared by machining one of the above flexures. Subtractive tools included waterjets, lasers, micro-milling systems, and additive tools such as laser powder bed fusion and 3D printers using metal and non-metal media. For this particular flexure, it should be pointed out that the geometry and/or materials of the flexure were not necessarily optimized for some of the machine tools.

The results of MicroCutting Project are partly summarized in Figure 3 in which aluminum flexures machined with both subtractive and additive tools are shown. The nominal size of the full-scale flexure was 60.7 mm (L) x 32.5 mm (W). The flexures were fabricated in different material thicknesses around 0.5 mm. Two additional flexures with 1/2 and 1/3 scales were also fabricated with several tools. The performance of the machine tools were evaluated by inspecting the geometries of the flexures under the microscope and observing the match/mismatch between the flexures and the tool path. Based on the test results, the performances of the  $\mu$ AWJ on the MicroMAX platform and the CNC micro milling conducted on the Zund G-3 L2500 stood out among all the tools investigated in the MicroCutting Project. For machining a single piece of flexure, the Zund took 2.5 min to machine part. The Zund performed slightly better than the MicroMAX in terms of part accuracy (element width and the uniformity along its axis) and edge quality (roughness and taper) (Liu and Gershenfeld, 2020).

For very thin materials, the OMAX PC-based CAM, MAKE, includes an optimum stack height calculator to estimate iteratively the optimum stack height that achieves the shortest cut time for the single sheet. As shown in Table 1, the AWJ using the 7/15 nozzle took 2.25 minutes to machine the flexure on a single sheet of 0.51 mm thick aluminum. The optimum number of sheets from the iteration to achieve the minimum time for one layer of 0.806 min was 11. The corresponding total stack thickness was 5.59 mm. As a result, there was a 2.79 times reduction in the cut time. In addition, there are two other benefits associated with of AWJ stack machining. First, the increase in the material thickness would effectively enable the activation of the TAJ for taper compensation. As a result, the taper for the individual sheets was minimized. Second, single sheets could be too delicate to be fixtured securely and firmly, degrading the cutting accuracy. The single sheets 7% of that of the EDM process (Liu, 2019a). During AWJ might be deformed under the load exerted onto the workpieces or distorted by the induced heat during machining. On the other hand, stack machining would not be an option for most CNC micromachining as the miniature spindles and end mills are too delicate to handle the increased load of the stack and the thickness-limited microlasers. For a detailed description of the above, refer to Liu and Gershenfeld (2020).

## 7 c) Macro to Micro Machining

In the early stage after the AWJ was commercialized, most R&D was focused on improving its performance in machining thick and difficult-to-cut materials to take advantage of its superior cutting power. Emphasis was made to engage in macro machining using relatively large nozzles and coarse abrasives at high feed rates. Metal parts such as aluminum and steel (annealed and/or hardened) around 0.20 m thick were routinely cut with AWJ (Liu and McNiel, 2010). An example is an AWJ-cut segment of a 1.52 m and 100 mm thick Bialloy gear of a wind turbine to replace a damaged counterpart below it, as shown in Figure 4. Also shown in the lower left of the figure is a portion of the damaged and AWJ-cut segments.

As the AWJ technology was maturing, R&D effort was subsequently shifted to improve the performance of AWJ for precision machining. Since AWJ is largely material independent, AWJ had progressively broadened the applications for machining most materials from metals, to nonmetals, and anything in between (Liu, 2017a). One of the important demonstrations was the success to apply AWJ to machine a simulated nanomaterial with large gradients of nonlinear material properties (Liu 2017b). The stack consisted of eight thin sheets of different materials including titanium, float glass, G-10 (black), aluminum, polycarbonate, stainless steel, carbon fiber, and copper. Based on the diverse properties of the individual materials, the stack possessed a wide range of properties from metallic to nonmetallic, conductive to non conductive, reflective to non reflective, and ductile

to brittle. There would be few conventional tools, if any, capable of machining such a stack. Meanwhile, smart digital control software was developed to streamline machining processes toward automation.

As described in Section 3.2, parallel effort was devoted to develop  $\mu$ AWJ technology for meso-micro machining with good success. In Figure 4 a  $\mu$ AWJ-cut miniature 3.5 mm planetary gear machined with the 5/10  $\mu$ AWJ nozzle was superimposed onto one of the teeth of the wind turbine gear; the miniature gear was merely shown as a speckle on the photograph. The striking size contrast in the two gears had demonstrated the capability of AWJ for machining features from macro to micro scales. Note that the cutting power of AWJ diminishes with the nozzle size. Table 2 compares the typical parameters used with the 5/10 and 10/21 nozzles. First of all, at the same pressure the hydraulic power and the water flow rate are proportional to the square of the orifice ID. In addition, the abrasive size ( $<1/3$  mixing tube ID) and abrasive feed rate ( $\sim 12\%$  of water by weight) must reduce according to the mixing tube ID. As a result, the typical mean abrasive particle size and feed rate reduce  $1/3$  and  $1/4$ , respectively. It is the combination of the reduction in the above parameters that leads to the diminishing of the cutting power. As such, the optimum material thickness reduces noticeably as the nozzle size decreases. For cutting thick materials, large nozzles with 10/21, 14/30, and 22/48 combination were preferably used for high productivity. The cold cutting and low side force exertion onto the work-piece by the  $\mu$ AWJ induced minimum mechanical and thermal distortion to the thin walls, preserving their designed shapes with no breakage. The average power of the solid-state laser pulsed at 5 kHz was about 6W. It induced no HAZ on the cut edges and no observed distortion on the walls. With a spot size of 50  $\mu$ m, it was able to cut the slots and walls accurately according to the designed dimensions. As such, the slots and walls were narrower and wider, respectively, for the solid-state laser cut butterfly than for the  $\mu$ AWJ and solid-state laser-cut counterparts. Pulsing the solid-state laser to minimize the HAZ resulted in slowing down the cut speed considerably. The cut time for the solid-state laser was about 60 minutes while that for the AWJ 5/10 nozzle was 2.2 min. In other words, the 5/10 nozzle cut 27 times faster than the solid-state laser did. The high-speed water not only accelerates the abrasive particles but also serves as the coolant. During AWJ cutting, the heat generated by the erosive mechanism of the abrasive is carried away by the spent water. As a result, the temperature at the cut edges only raised moderately to around 80°C or less particularly when a chiller is used (Jerman, et al., 2011). On the other hand, the induced heat by lasers cutting and EDM was so high that they must slow down the cutting speed significantly to minimize the heat-affected zone (HAZ). The remedies were to pulse Lasers at high frequencies (e.g. solid-state lasers) and apply thin wire EDM to cut with multiple passes. For heat sensitive materials, therefore, AWJ is capable of cutting at speeds about one order of magnitude faster than lasers and EDM (Liu, 2019a; Liu and Gershenfeld, 2020). Other thermalbased machine tools such as plasma and oxyfuel cutters induced so much HAZ for cutting stainless steel and hardened steel that results in surface hardening and reduces the weld integrity of the workpiece. The HAZ must be removed by secondary processes such as grinding (Wright, 2016). The secondary process of grinding is often time consuming and labor intensive, particularly for very large structure such as shells of spherical pressure vessels made from stainless steel or hardened steel.

For thermal or mechanical-based machine tools, the high heat or large side force distorts the parts during machining. Such distortions may lead to permanent blemishes on the parts. In collaboration with the Center of Bits and Atoms at Massachusetts Institutes of Technology, the performances of a CO<sub>2</sub> and a solid-state lasers with the 5/10  $\mu$ AWJ nozzle were compared by machining a miniature butterfly on 0.5 mm thick stainless steel. Figure 5 shows three photographs of the laser-and  $\mu$ AWJ-cut parts. It is evident that the heat generated by the CO<sub>2</sub> laser led to evaporate most of the material. The  $\mu$ AWJ-cut butterfly shows that the kerf width of about 280  $\mu$ m was slightly too large to negotiate the narrow slots that are wider than the designed width of these slots. As a result, the walls between the slots are thinner than their designed width.

The MIT Precision Engineering Research Group ([www.pergr.com](http://www.pergr.com)) has developed flexure-based nonlinear load cells, with 1% change in the force and five orders of magnitude in the force range (MIT US Patent #20150233440). There were two designs of the load cells consisted of large-aspect-ratio thin flexures with constant and variable width, respectively (Kluger et al., 2016; Kluger et al., 2017). The constant taper load cell consisted of four 1 mm wide flexure straight elements with an aspect ratio (length to width) of 98.3. The tapered load cell consisted of four tapered ring-shaped flexures with a diameter of 19.1 mm. The taper began and ended with widths of 10 mm and 0.5 mm. The narrow gaps between the flexures and the frames of the load cells were 1.06 mm and 0.42 mm, respectively. There was considerable challenge in machining the load cells made from 6.35 mm thick 6061T6 aluminum because of their geometries and tight tolerances. Note that lasers were not efficient in cutting the aluminum with high thermal conductivity; EDM was expected to be too slow because it must cut via multiple passes to minimize the HAZ; and CNC milling must cut slowly to avoid the mechanical distortion of the high aspect-ratio thin flexures. The flexures were subsequently machined with the  $\mu$ AWJ to take advantage of its capability of cold cutting and low side force exertion to the workpiece. Machining was successfully conducted using the 7/15 nozzle with 240 mesh garnet. The Tilt A-Jet was activated to minimize the edge taper. Figure 6 shows photographs of the two  $\mu$ AWJ machined nonlinear load cells. Their performances were verified through laboratory tests conducted at MIT (Kluger et al., 2016; Kluger et al., 2017). One of the essential criteria for the success in the verification of their performances was that the edge taper on the flexure element must be minimized. The software's IntelliTaper process was utilized to minimize the edge taper. Machined aluminum coupons that were 51 mm long x 12.7 mm width x 6.35 mm thick, the same thickness as the load cells, showed that the average edge taper of the two sides on the coupon was reduced to 0.03 degree. (Liu, 2016). Figure 7a is a micrograph of

one of the four flexures shown in Figure 6a with the superimposition of the corresponding tool path. Excellent match between the  $\mu$ AWJ-machined part and the tool path is observed. The constant-width and tapered flexures were also machined with CNC milling on a Haas UMC750 with a 6.35 mm end mill, as shown in Figure 7b. Since the diameter of the end mill is larger than the gaps between the flexures and the frame of the load cells, the above setup would be unable to machine the load cells. Modifications of the flexures by enlarging the gaps were made to accommodate the large end mill. The CNCmilled constant-width flexure shown in Figure 7b was bent slightly either due to the side force exerted by the end mill on the flexure or the excessive heat induced during milling (Liu, 2019a). Besides, a part of the flexure did not cut through its full depth. The above findings demonstrated that the cold cutting and low side force exertion of the AWJ are import factors in achieving the part accuracy and structural integrity for meso-micro machining. Year 2020 As a material independent tool, AWJ has been applied to drill holes on most materials ??Liu, 2016a ??Liu, , 2016b)). Since the AWJ cuts with erosive mechanism, it is largely material independent. Note that lasers and EDM are material restrictive because they are incapable of cutting reflective material with high conductivity and conductive materials, respectively. As a flexible cutting/drilling tool, AWJ does not drill straight walled holes but with specific geometries that vary with the materials (Liu, 2006b). Figures 8a and 8b show photo-graphs of two sets of holes drilled with the AWJ at  $p = 241$  MPa on aluminum and float glass, respectively. The overall geometries of these holes are similar except at the hole entry. The difference in geometries, as can be observed in the profiles of the holes shown in Figures 8a and 8b is attributed to the difference in the material properties and the wear resistance. Note that the float glass and aluminum are brittle and ductile materials with machinability numbers of  $M = 350$  and  $215$ , respectively. During drilling blind holes, the return slurry (Liu, 2006b) flow when exiting the entry holes wears the glass more than the aluminum. As a result, the glass hole entry was rounded to form a funnel shape. Figure 9a presents the profiles of the holes measured from the photographs shown in Figure 8. By scaling the hole depth,  $l$ , with the The profiles shown in Figure 9a were reasonably collapsed as demonstrated in Figure 9b. As a result, the dependency on drill time was minimized. Note that the left-hand-side of the equation would become non dimensional provided the drill time is multiplied by the drill speed. However, the drill time was not monitored at that time. For an in-depth study of AWJ drilling in ductile materials such as aluminum and mild steel, empirical modeling by means of nonlinear regression methods was conducted to include a wide range of relevant parameters including pump pressure abrasive flow rate, material thickness, dwell time, and nozzle combination (Liu, 2006c). Early attempts to pierce delicate materials such as composites and laminates with AWJ had failed due to cracking, delamination, and chipping. Considerable R&D was devoted to investigate the causes of the phenomenon. Based on a CFD simulation in drilling holes with AWJ, it was determined that the damage was attributed to the buildup of stagnation pressure during the initial piercing stage before breakthrough (Liu et al., 1998;Liu, 2006a). As the high-speed waterjet jet enters the blind hole, it decelerates, stops, and reverses its course. At the stagnation point near the bottom of the blind hole, the kinetic energy of the waterjet largely converts into the potential energy in the form of the stagnation pressure (Bachelor, 1967). Damage takes place when the stagnation pressure exceeds the tensile strength of the delicate materials.

One of the remedies was to minimize the buildup of the stagnation pressure inside the blind hole. Subsequently, abrasive cryogenic jet (ACJ) and the patented flash abrasive waterjet (FAWJ) were developed by using liquefied nitrogen and super-heated water as working fluids to accelerate the abrasives (Liu, 2006b;Liu and Schubert, 2009). Most of the liquefied nitrogen of the ACJ and the superheated water of the FAWJ evaporated upon exiting the nozzles leaving mainly the accelerated abrasives entering into the blind holes. As such the buildup of the stagnation pressure was minimized and piercing damage of delicate materials was mitigated. However, both the ACJ and the FAWJ were not practical tools for industrial applications as the working fluids were too aggressive for the components of the high-pressure pump and accessories. Based on the understanding derived from the test results of the ACJ and the FAWJ, proprietary processes were successfully developed to modify the AWJ through pressure control during piercing . Two proprietary processes, a TurboPierce and a MiniPierce, were developed and applied to pierce large and small holes, respectively.

Figure 10 illustrates photographs of aluminum laminate samples (BAC1534-63F) pierced with the TurboPierce process. The laminate consisted of 19 aluminum sheets 0.076 mm thick with an overall thickness of 1.6 mm. The laminate was formed by stacking the sheets together with adhesive between sheets. Most adhesives do not have very strong adhesive strength. If the stagnation pressure developed inside the blind hole during piercing exceeds the adhesive strength, delaminate would result. The 14/42 nozzle with 80 mesh garnet were used in cutting the internal features on the samples. Piercing was carried out by slightly pressurizing the abrasive hopper. Cutting was performed at  $p = 380$  MPa. The photo-graphs shown in Figures 10a and 10b correspond to the samples machined before and after the TurbPiercer was optimized, respectively. The left photograph showed delamination around most of the holes. The most serious damage was observed on the right most three holes with a large delamination bubble covered all three holes. There is however no sign of any delamination on the right photograph. The effectiveness in mitigating delamination of the optimized Turbo Piercer was evident. For thin workpieces such as the 0.076 mm individual shims of the aluminum laminate, as discussed in Section 3.2, the optimum way to machine them with AWJ was through stack cutting. The top and bottom shims of the stack would serve as the sacrificial covers to protect the interior ones from frosting (top shim) and burring (bottom shim). After the stack is cut, the internal shims would be nearly identical with no frosting and burr, as illustrated in Figure 11b.

For modern aircraft engines operating at a very high temperature, there is need for drilling inclined and shaped air breathing holes to achieve efficient and maximum cooling. The current practice requires a twostep process to drill inclined and shaped holes on TBC. For cutting small internal features on the aluminum laminate described above, the Mini Piercer with a 5/10 nozzle was used. In this case, pressures of 41 MPa and lower were required to mitigate delamination. For such low pressures, the Venturi vacuum developed after the waterjet exits the orifice was too weak to entrain all the abrasives fed from the hopper. Vacuum assist was required to enhance the vacuum level while removing excessive abrasives accumulated in the mixing chamber. Otherwise, the mixing tube would be clogged by the excessive abrasives. As soon as breakthrough took place, normal high-pressure cutting at 380 MPa resumes to cut the features at high speeds. Figure 11a First, the nonconductive TBC is re-moved with a laser and the hole in the substrate is drilled with an EDM process. The versatile AWJ was one of the suitable tools to drill such holes on refractory metals with and without a thermal barrier coating (Liu et al., 2018b). By mounting the workpiece on the Rotary Axis, any inclined angle of the holes can be drilled. The geometries of the holes were drilled by controlling the tilting of the A-Jet. Within a certain limitation, the inclined angle and the shape can vary simultaneously along the hole axis. The process involved drilling through the thermal barrier coating at low pressures and then followed by drilling into the refractory metal at high pressures. As such, delamination in the delicate thermal barrier coating was mitigated while accelerating the drilling in the difficult substrate without the HAZ (Liu, 2017a).

f) Gear Making AWJ has been used extensively for machining gears, racks, and sprockets. Examples of gear from macro to micro scale are shown in Figures 1 and 4. The OMAX PC-based CAD program, LAYOUT, has a gear command for creating a variety of gears and racks. A gear command creates a drawing exchange format (dxf) file by choosing the options of the gear (external or internal), rack, or sprocket, and defining the number of teeth, pitch, and pressure angle. For special gears, an option is to import a CAD drawing to the PC-based LAYOUT to create the tool paths to run in MAKE. Additional examples are shown in this section to demonstrate the versatility of AWJ for machining gears made from several materials for various applications.

One of the interesting projects was to machine a wood clock with the AWJ and then assembled the parts into a working one. There were many choices of design available from a number of websites. The Genesis that was simple but elegant was selected (Boyer, 2018). The complete plan in the dxf file was available online. All the components of the Genesis clock mostly made of high-density plywood with thicknesses ranging from 3.2 mm to 19.1 mm were then cut on a MAXIEM waterjet system in the OMAX Demo Lab. It took just hours to cut all the components with high accuracy as opposed to days using a scroll saw. Figure 12 shows the assembled wood clock. The faces of the hour (lower left), minute (middle), and second (right) gears were cut from a thin stainless-steel sheet rather than cutting the individual numbers from wood or engraving them onto the wheels. The clock was controlled by the adjustable length of the pendulum; it was calibrated with an electric clock. The clock was driven by a 3.2 kg stainless steel round bar that turned a click wheel attached to the back of the minute gear via a fish line. A small aluminum round bar serves as the counter balance to straighten the fish line as the clock runs. The assembled clock ran well with a pleasant clicking sound as designed (Boyer, 2018).

A miniature planetary gear set made of titanium sheet 0.25 mm thick was machined on the MicroMAX using the 5/10 nozzle with the 320 mesh garnet. Figure 13 shows the photographs of the nested components and the assembled planetary gear. Also shown in Figure 13a is a part of the nested tool paths; the tool paths of the center and ring gears were cut coaxially on the material. The same set of gears were machined on stainless steel, and Polyether Ether Ketone (PEEK) without and with reinforced fibers to demonstrate the material independence of AWJ machining.

## 8 Summary

In this paper, AWJ-machined samples were presented to demonstrate the versatility of waterjet technology for macro to micro machining for a wide range of materials. Part 1 of the paper emphasizes six particular areas to take advantage of the technological and manufacturing merits of waterjet technology:

- ? Smart controller software that is smart and intuitive but powerful.
- ? Meso-micro and stack machining through the development of  $\mu$ AWJ technology and downsizing of AWJ nozzle.
- ? Macro to micro machining that is carried out with a single tool using several sizes of nozzle and abrasives on JetMachining Center with a wide range of work envelopes.
- ? Cold cutting together with exertion of low side force on workpieces that induces no heat-affected zone while preserving the structural integrity of parent materials.
- ? Hole drilling on both difficult and delicate materials.
- ? Gear making for a wide range of geometries and sizes on various materials. Based on the above applications, the versatile AWJ/ $\mu$ AWJ technology has established and will set new trends in advanced manufacturing. One of the established trends that has the most impacts on the manufacturing industry is its "7M" advantage, that is, multimode machining of most materials from macro to micro scales (Liu, 2017a). Specifically, all it takes is a single tool using different sizes of nozzles, abrasives, and JetMachining platforms to achieve the above. The "7M" advantage can be applied to a wide range of precision machining:
- ? AWJ relies on erosion by high-speed abrasives. It is largely material independent and is capable of machining both delicate and difficult-to-machine materials from metals to nonmetals and anything in between. It is even

capable of machining nanomaterials with large gradients of nonlinear material properties that present considerable challenge to conventional machine tool (Liu, 2017b) ? Macro machining using large nozzles and coarse abrasives with high feed rates on JMCs with large work envelopes to machining both delicate and difficult materials o Delicate materials include glass (except highly tempered ones), composites, laminates, and others o Difficult materials include refractory metals, various alloys (such as Inconel, tungsten, and Titanium), tool/hardened steel, and others o Cut stainless steel 0.2 m and thicker

? Meso-micro machining of most materials Although the current production and experimental  $\mu$ AWJ nozzles are capable of machining feature as fine as 200  $\mu$ m, cold cutting with low side force exertion on workpieces enables machining very thin wall (<100  $\mu$ m) between features o For relatively soft materials, water-only jets are capable of machining features <100  $\mu$ m.

o Stack machining is expected to be most advantageous for micromachining as it ? Serves as "self fixturing" through stiffening individual shims that are difficult to fixture and machine otherwise ? Increases productivity through machine multiple nearly identical parts at optimum cut time for individual shims ? Increases overall thickness enabling activation the TAJ to achieve minimum taper of individual shims

In Part 2 of the paper, additional examples of AWJ/ $\mu$ AWJ machining will be presented to complete the description of recent advancements in the technology. The paper in its entirety will enable to describe the established and new trends of AWJ technology in advanced manufacturing.

1 2 3 4 5 6 7 8 9 10

---

<sup>1</sup>For very thin materials, the Tilt-A-Jet is deactivated as the cutting speeds are too fast such that the Tilt-A-Jet is too slow

<sup>2</sup>Review of Accomplishments in Abrasive-Waterjet from Macro to Micro Machining -Part 1 © 2020 Global Journals

<sup>3</sup>© 2020 Global Journals

<sup>4</sup>Review of Accomplishments in Abrasive-Waterjet from Macro to Micro Machining -Part 1

<sup>5</sup>Beam Dynamics Model LMC10000 CO 2 laser system (500W) and Oxford Solid State Micro Machining Laser -532nm diodepumped solid-state laser (6W at 10 kHz).

<sup>6</sup>© 2020 Global Journals a. Constant-width flexures b. Tapered flexures Review of Accomplishments in Abrasive-Waterjet from Macro to Micro Machining -Part 1 © 2020 Global Journals

<sup>7</sup>© 2020 Global Journals a. Profiles b. Scaled profiles

<sup>8</sup>© 2020 Global Journals Review of Accomplishments in Abrasive-Waterjet from Macro to Micro Machining -Part 1

<sup>9</sup>a. Components and tool paths b. Assembled

<sup>10</sup>Year 2020 © 2020 Global Journals





1

Figure 1: Figure 1 :

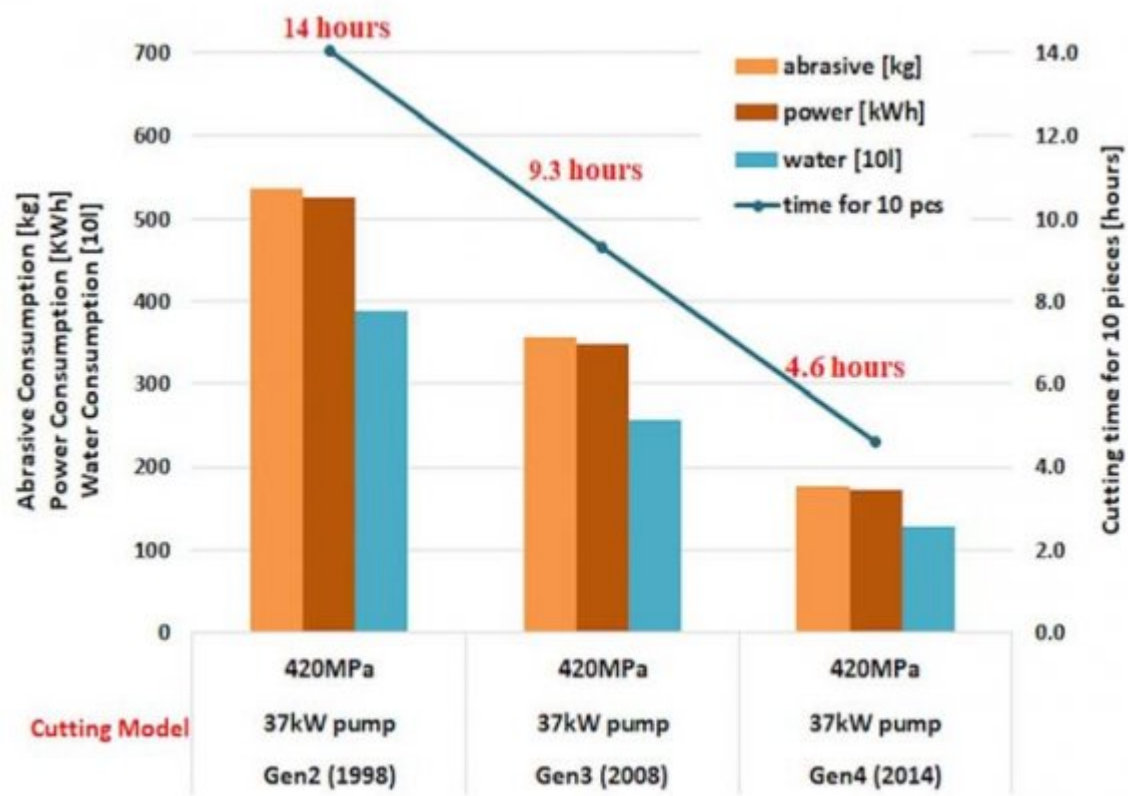


Figure 2:

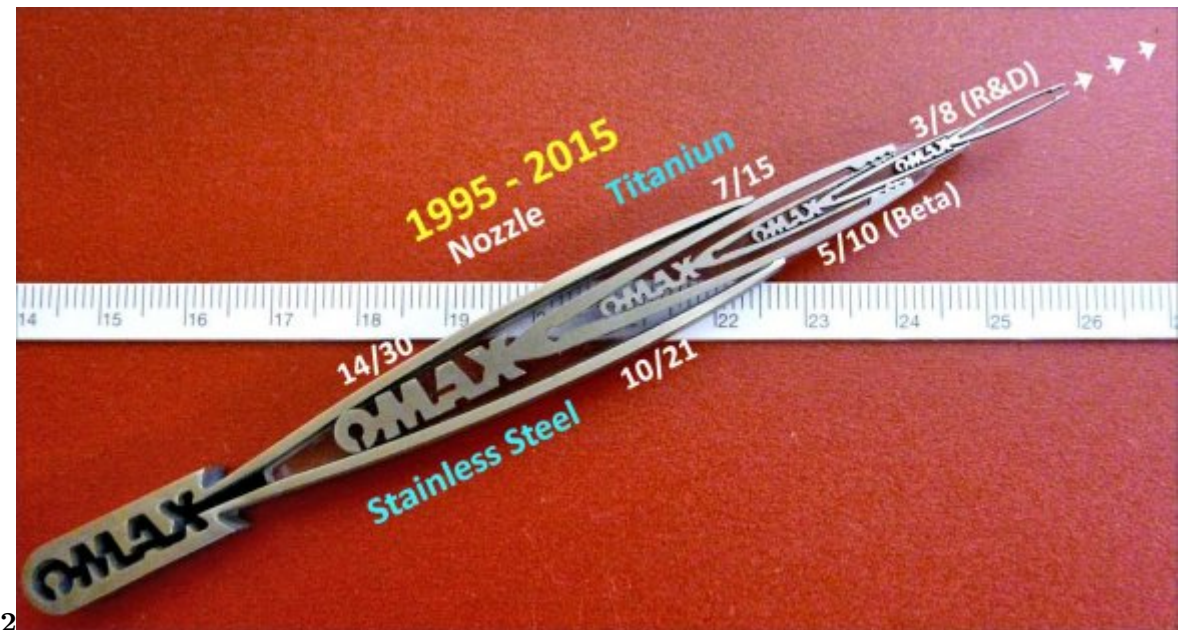


Figure 3: Figure 2 :

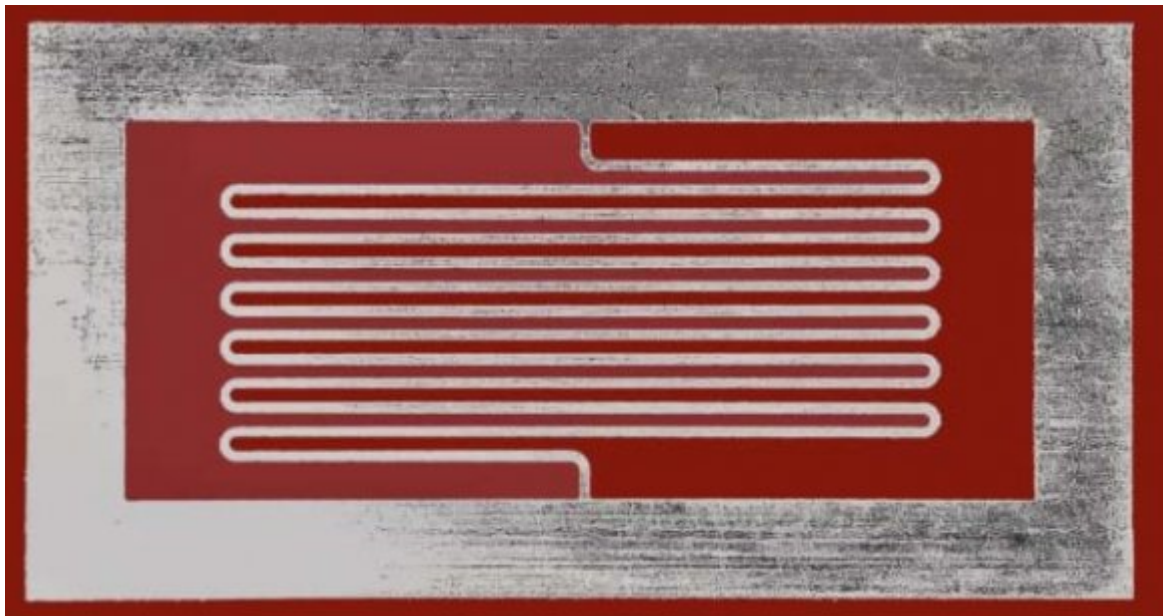
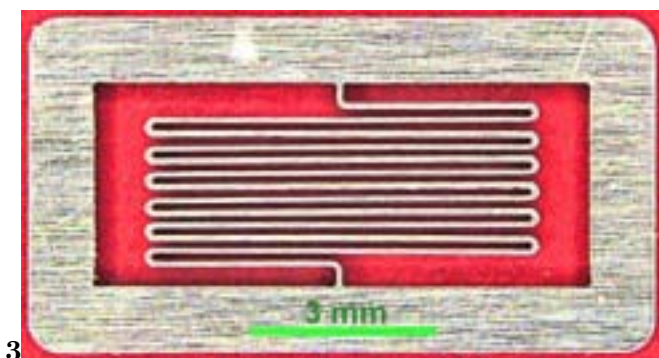


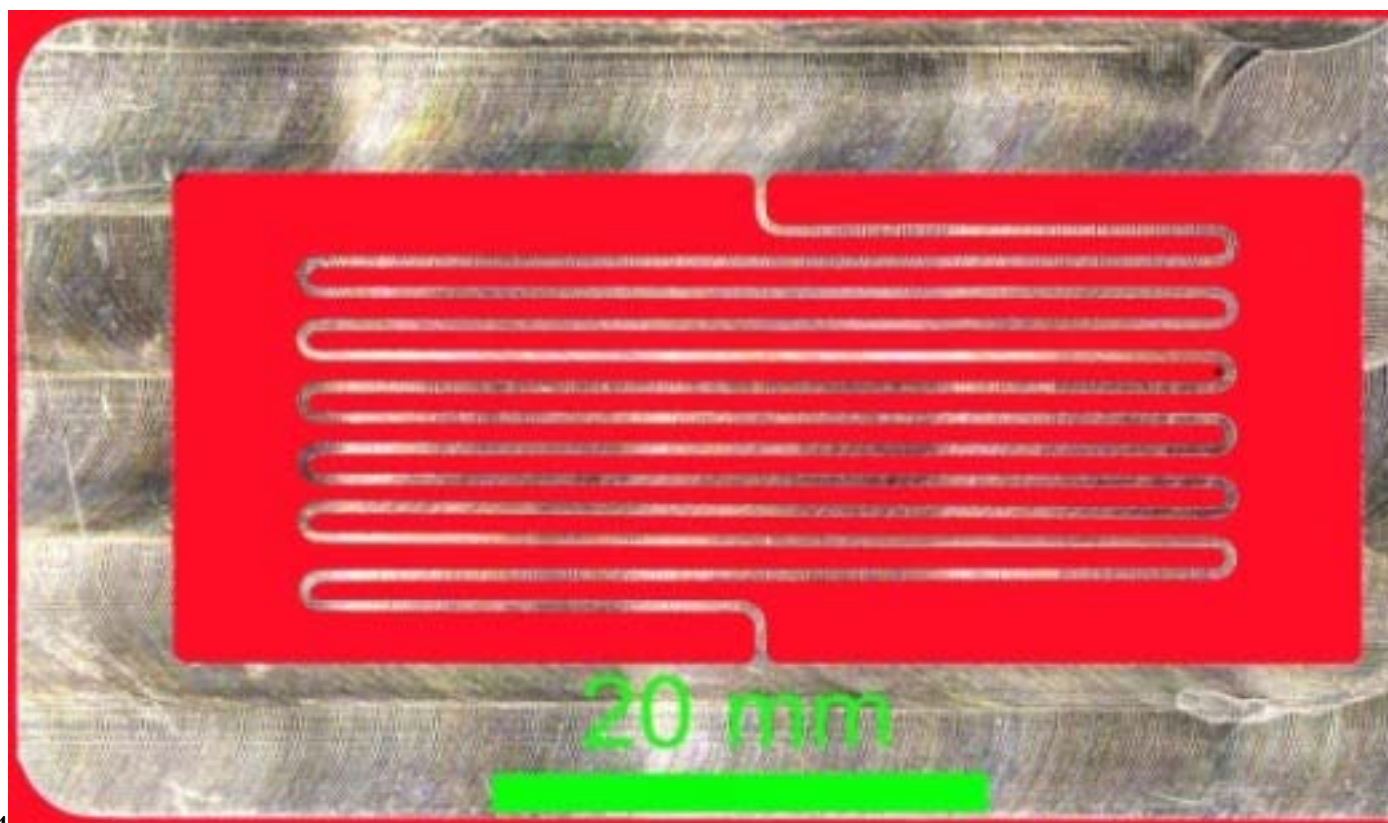
Figure 4:



3

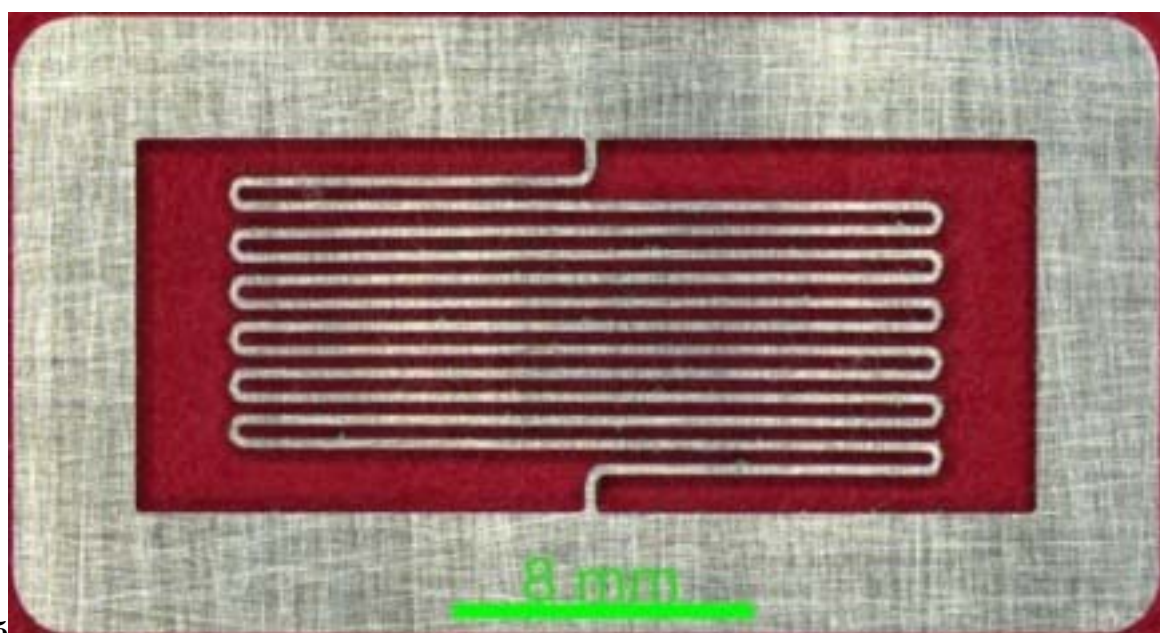
Figure 5: Figure 3 :





4

Figure 6: Figure 4 :



5

Figure 7: Figure 5 :

6

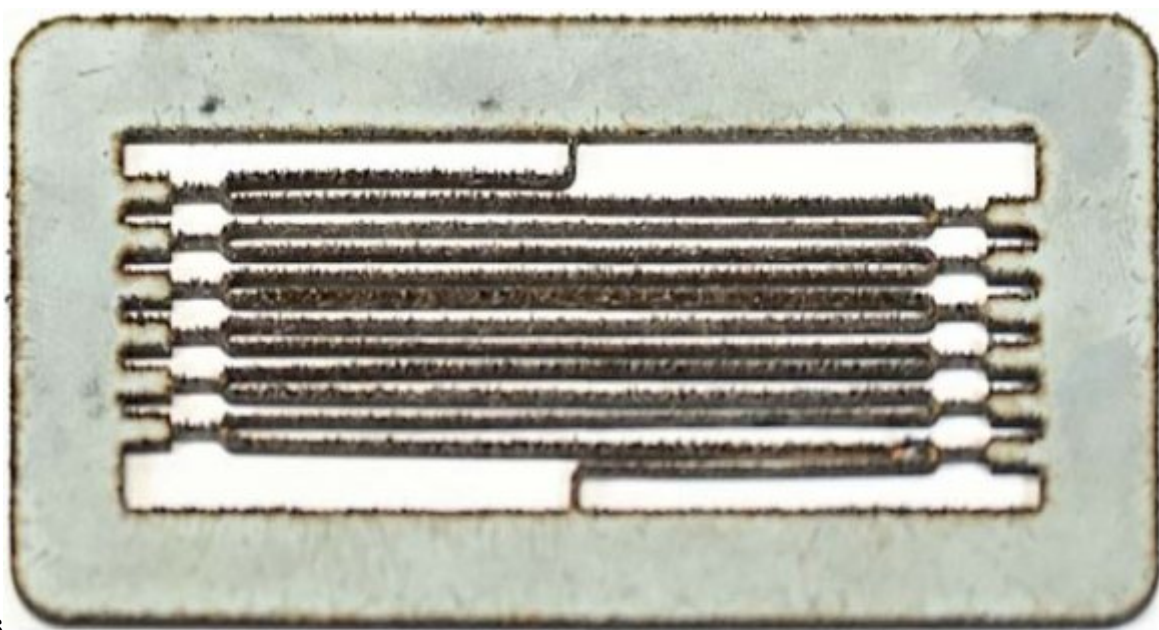


Figure 8: Figure 6 :

7

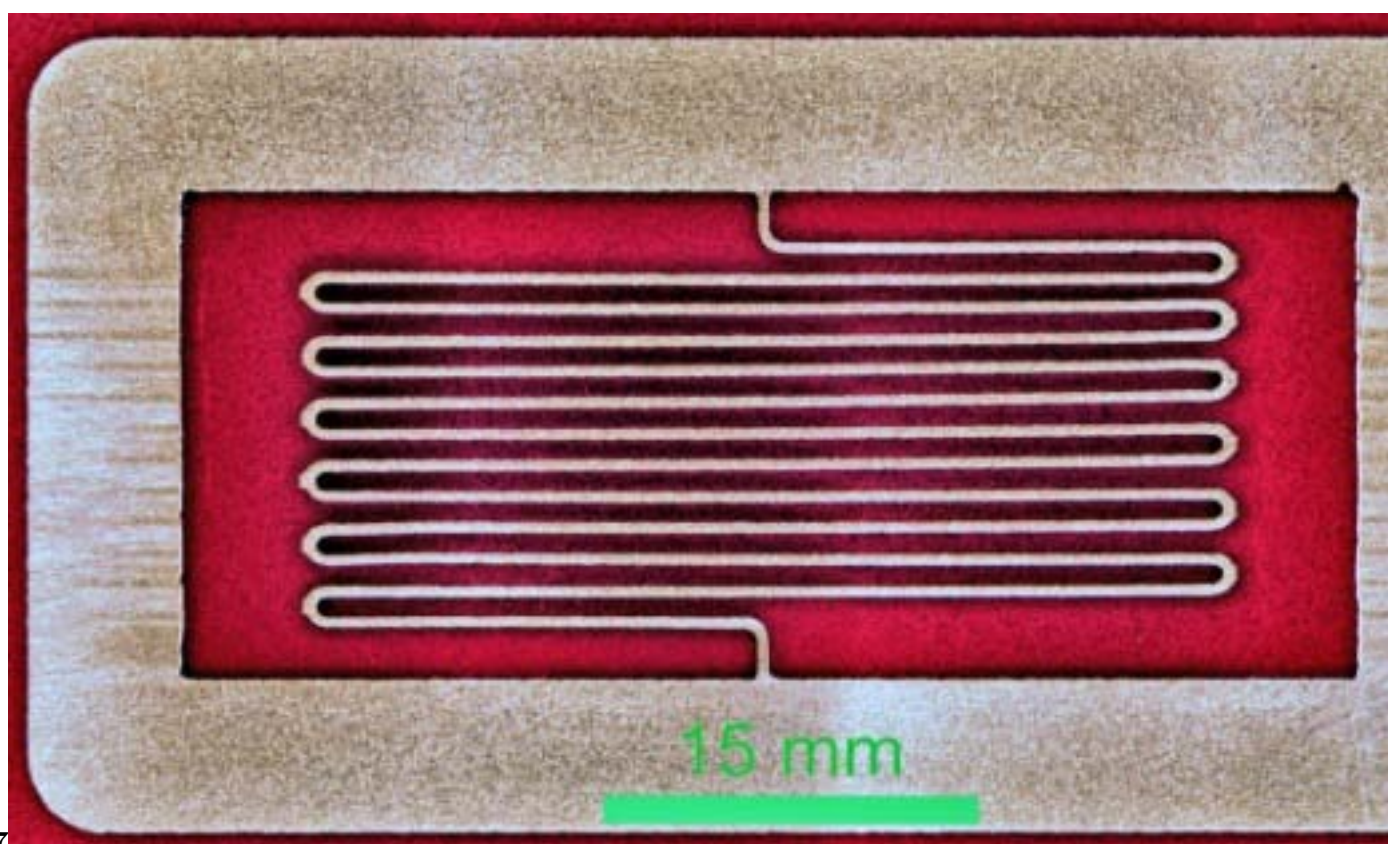


Figure 9: Figure 7 :



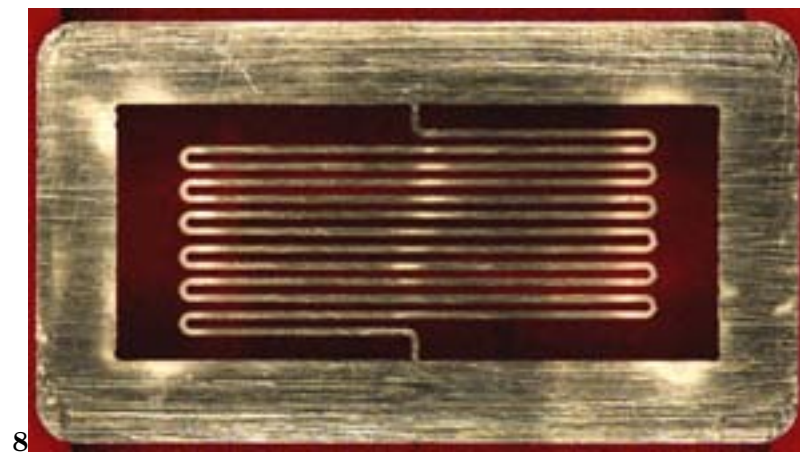


Figure 10: Figure 8 :

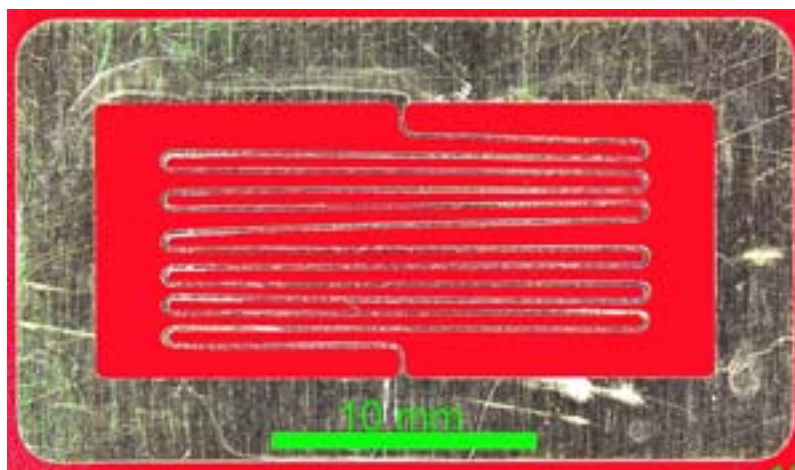


Figure 11:



Figure 12: Figure 9 :

10



Figure 13: Figure 10 :



11

Figure 14: Figure 11 :



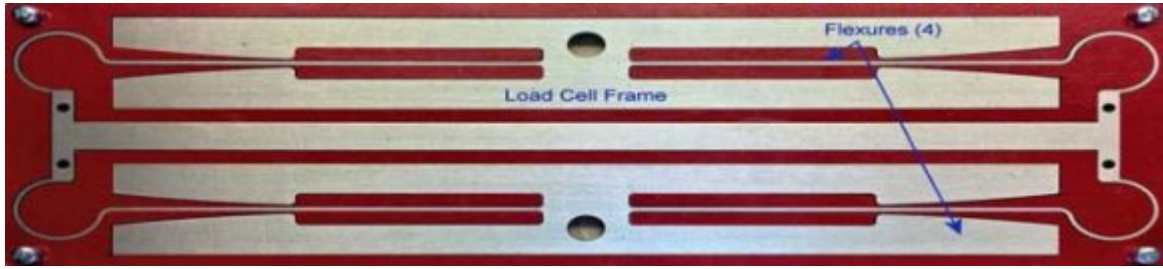
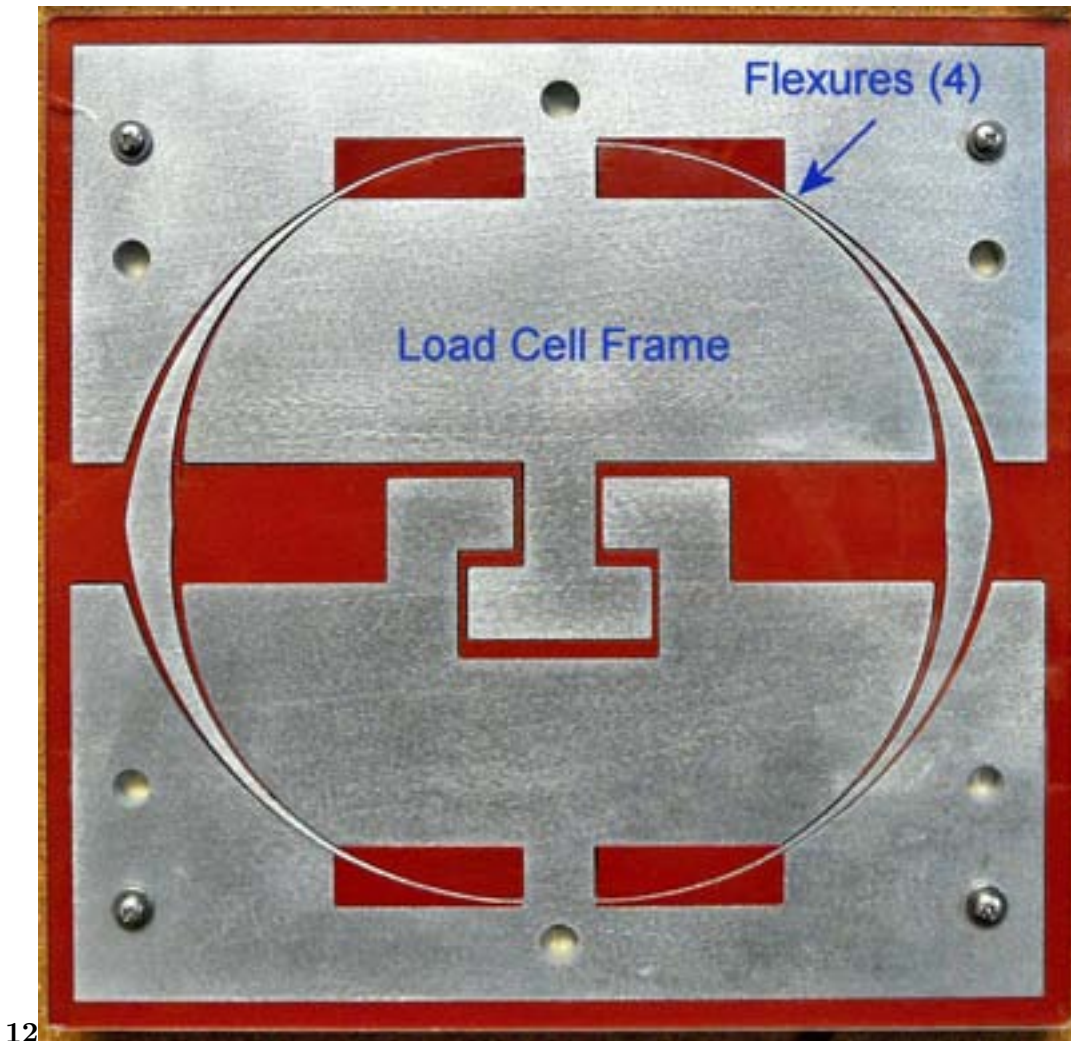


Figure 15:



12

Figure 16: Figure 12 :

$$\frac{d(l)}{\ln(t)} = f\left(\frac{l}{l_{max}}\right),$$

13

Figure 17: Figure 13 :

1

| Number<br>of Sheets<br>in Stack | Time for Stack (min) | Time For one Layer<br>(min) | Total Thickness |
|---------------------------------|----------------------|-----------------------------|-----------------|
| 1                               | 2.2455               | 2.2455                      | 0.02/0.51       |
| 2                               | 2.5879               | 1.2939                      | 0.04/1.02       |
| 3                               | 3.0557               | 1.0186                      | 0.06/1.52       |
| 4                               | 3.6441               | 0.9110                      | 0.08/2.03       |
| 5                               | 4.2408               | 0.8482                      | 0.10/2.54       |
| 6                               | 4.9268               | 0.8211                      | 0.12/3.05       |
| 7                               | 5.6523               | 0.8075                      | 0.14/3.56       |
| 8                               | 6.4519               | 0.8065                      | 0.16/4.06       |
| 9                               | 7.2732               | 0.8081                      | 0.18/4.57       |
| 10                              | 8.0696               | 0.8070                      | 0.20/5.08       |
| 11                              | 8.8651               | 0.8059                      | 0.22/5.59       |
| 12                              | 9.7329               | 0.8111                      | 0.24/6.10       |

Figure 18: Table 1 :

2

| Orifice ID<br>(in/mm) | Pressure<br>(ksi/MPa) | Hydraulic Power<br>(hp/kW) | Flow Rate<br>(gpm/l/min) | Abrasive Feed Rate<br>(lb/min/g/min) | Abrasive and<br>Mean Size<br>(Mesh/ $\mu$ m) | Standoff<br>Distance<br>(in/mm) |
|-----------------------|-----------------------|----------------------------|--------------------------|--------------------------------------|--|---------------------------------|
| 0.005/0.127           | 55/379                | 3.7/2.7                    | 0.11/0.53                | 0.10/26                              | 240/60                                       | 0.03/0.76                       |
| 0.010/0.254           | 55/379                | 15/11                      | 0.44/2.1                 | 0.35/92                              | 80/250                                       | 0.06/1.52                       |

Figure 19: Table 2 :

- [Boyer and Genesis ()] , C Boyer , Genesis . <http://lisaboyer.com/Claytonsite/Genesisispage1.htm> 2018.
- [Liu ()] '7M" Advantage of Abrasive Waterjet for Machining Advanced Materials'. H.-T Liu . <https://www.mdpi.com/2504-4494/1/1/11> *J. Manuf. Mater. Process* 2017a. MDPI. 1 (1) .
- [Liu ()] 'Advanced Waterjet Technology for Machining Curved and Layered Structures'. H.-T Liu . <https://www.degruyter.com/downloadpdf/j/cls.2019.6.issue-1/cls-2019-0004/cls-2019-0004.pdf> *Curled and Layer Structure Journal* (Online) 2353-7396. 2019b. Peter. 6 (1) p.
- [Wright (2016)] *An Engineer's Guide to Waterjet Cutting*, I Wright . [https://www.engineer-ing.com/AdvancedManufacturing/ArticleID/12716/An-Engineers-Guide-to-Waterjet-Cutting.aspx#disqus\\_thread](https://www.engineer-ing.com/AdvancedManufacturing/ArticleID/12716/An-Engineers-Guide-to-Waterjet-Cutting.aspx#disqus_thread) 2016. July. (Manufacturing)
- [Bachelor ()] *An Introduction to Fluid Dynamics*, G K Bachelor . 1967. London: Cambridge University Press. p. 285.
- [Liu et al. (1998)] 'CFD and Physical Modeling of UHP AWJ Drilling'. H.-T Liu , P Miles , S D Veenhuizen . *Proc. 14 th Int. Conf. on Jetting Technology*, (14 th Int. Conf. on Jetting TechnologyBrugge, Belgium) 1998. September 21 -23. p. .
- [Liu (2006)] 'Collateral Damage by Stagnation Pressure Buildup during Abrasive-Fluidjet Piercing'. H.-T Liu . *Proc. 18 th Int. Conf. On Water Jetting*, (18 th Int. Conf. On Water JettingGdansk, Poland) 2006a. September 13-15.
- [Henning and Miles (2016)] 'Conservation of Energy Drives Cutting Performance'. A Henning , P Miles . *Proc. of the 23 rd Int Conf on Water Jetting*, (of the 23 rd Int Conf on Water JettingSeattle, WA) 2016. November. p. .
- [cteristics-and-applications/advanced-abrasive-water jet-for-multimode-machining)] *cteristics-and-applications/advanced-abrasive-water jet-for-multimode-machining*),
- [Zeng ()] *Determination of machinability and abrasive cutting properties in AWJ cutting*, J Zeng . 2007. 2007.
- [Miller (2003)] 'Developments in Abrasive Waterjets for Micromachining'. D S Miller . *Proc. 2003 WJTA Amer. Waterjet Conf*, (2003 WJTA Amer. Waterjet ConfHouston, Texas) 2003. August 2003. (Paper 5-F. 17-19)
- [Liu (2006)] 'Empirical Modeling of Hole Drilling with Abrasive Waterjets'. H.-T Liu . *Proc. 18 th Int. Conf. On Water Jetting*, (18 th Int. Conf. On Water JettingGdansk, Poland) 2006c. September 13-15.
- [Liu ()] 'Hole Drilling with Abrasive Fluidjets'. H.-T Liu . 10.1007/s00170-005-0398-x). *Int. J. of Adv. Manuf. Tech* 2006b. 32 p. .
- [Tate (2013)] *How to Catch an Asteroid: NASA Mission Explained (Infographic)*, K Tate . 2013. April.
- [Xu et al. ()] 'Investigation on characterization of powder flowability using different testing methods'. G Xu , P Lu , M Li , C Liang , P Xu , D Liu , Chen , Xi . *Experimental Thermal and Fluid Science* 2018. 92 p. .
- [Jerman et al. (2011)] 'Measuring the Water Temperature Changes throughout the Abrasive Waterjet Cutting System'. M Jerman , H Orbanic , I Etxeberria , A Suarez , M Junkar , A Lebar . *Proc 2011 WJTA-ICMA Conference and Expo*, (2011 WJTA-ICMA Conference and ExpoHouston, Texas) 2011. September 19-21.
- [Liu and Schubert (ed.) (2012)] *Micro Abrasive-Waterjet Technology (Chapter Title)", Micromachining Techniques for Fabrication of Micro and Nano Structures*, H.-T Liu , E Schubert . <http://cdn.intechweb.org/pdfs/27087.pdf> Mojtaba Kahrizi (ed.) 2012. January. INTECH Open Access Publisher. p. .
- [Miller (2005)] 'New Abrasive Waterjet Systems to Complete with Lasers'. D S Miller . *Proc. 2005 WTJA Amer. Waterjet Conf*, (2005 WTJA Amer. Waterjet ConfHouston, Texas) 2005. August 21-23. p. .
- [Liu and Peter ()] 'Novel Processes for Improving Precision of Abrasive-Waterjet Machining'. Liu , ) H.-T Peter . *Proc 2015 WJTA-ICMA Conference and Expo*, (2015 WJTA-ICMA Conference and ExpoNew Orleans, Louisiana) 2015. November 2-4.
- [Liu and Peter ()] 'Novel Processes for Improving Precision of Abrasive-Waterjet Machining'. Liu , ) H.-T Peter . *Proc. 2015 WJTA-ICMA Conference and Expo*, (2015 WJTA-ICMA Conference and ExpoNew Orleans, Louisiana) 2015. November 2-4.
- [Liu et al. ()] 'Performance comparison of subtractive and additive machine tools for meso-micro machining'. Liu , ) H.-T Peter , Neil Gershenfeld . <https://www.mdpi.com/2504-4494/4/1/19/pdf> *J. Manuf. Mater. Process. (JMMP)* 2020. MDPI. 4 (1) .
- [Liu ()] 'Performance Comparison on Meso-Micro Machining of Waterjet, Lasers, EDM, and CNC Milling'. H.-T Liu . <http://ijeert.org/papers/v7-i6/4.pdf> *International Journal of Emerging Engineering Research and Technology* 2349-4395(print) and 2349-4409 (Online) DOI: i6. 2019a. 2019. Peter. 7 (6) p. .
- [Liu and Schubert ()] 'Piercing in Delicate Materials with Abrasive-Waterjets'. H.-T Liu , E Schubert . 10.1007/s00170-008-1583-5. *Int. J. of Adv. Manuf. Tech* 2009. 42 (3-4) p. .

- [Liu ()] 'Precision machining of advanced materials with abrasive waterjets'. H.-T Liu . 10.1088/1757-899X/164/1/012008/pdf. 164. 012008. <http://iopscience.iop.org/article/10.1088/1757-899X/164/1/012008/pdf> *IOP Conf. Series: Materials Science and Engineering*, 2017c.
- [Proc. Amer. WJTA Conf. and Expo ()] *Proc. Amer. WJTA Conf. and Expo*, (Amer. WJTA Conf. and Expo-Houston, Texas) August 19-21, 2007.
- [Zeng et al. ()] 'Quantitative fvaluation of machinability in abrasive waterjet machining'. J Zeng , T J Kim , R J Wallace . *Proc. of 1992 Winter Annual Meeting of ASME, Precision Machining: Technology and Machine Development and Improvement*, (of 1992 Winter Annual Meeting of ASME, Precision Machining: Technology and Machine Development and ImprovementAnaheim) 1992. 1992. 58 p. .
- [Liu et al. (2018)] 'Recent Advancement in Abrasive Waterjet for Precision Multimode Machining'. Liu , ) H.-T Peter , V Cutler , N Webers , ) H.-T Peter , V Cutler , C Raghavan , P Miles , N Webers . <https://www.intechopen.com/books/abrasive-technology-chara> *Abrasive Technology -Characteristics and Applications*, (Manchester, UK; Ed. Anna Rudawska) 2018a. September 5-7. Liu. 2018b. October. Intech Open Publisher. 978 p. . (Proc. 24 th Int. Conf. on Water Jetting)
- [Liu and Peter ()] 'Roles of taper compensation in AWJ precision machining'. Liu , ) H.-T Peter . *Proc. 23 rd Int. Conf. on Water Jetting*, (23 rd Int. Conf. on Water JettingSeattle, WA, Nov) 2016. p. .
- [Yadav and Singh (2016)] 'Study on water jet machining and Its future trends'. G S Yadav , B K Singh . *International Journal of Recent Research Aspects* 2349-7688. 2016. June. 3 (2) p. .
- [Liu ()] *Versatility of micro abrasive waterjet technology for machining nanomaterials*, H.-T Liu . 10.1081/E-ENN3-120054064. 2017b. p. . (Dekker Encyclopedia of Nanoscience and Nanotechnology)
- [Liu and Mcniel (2010)] 'Versatility of waterjet technology: from macro and micro machining for most ma-terials'. H.-T Liu , D Mcniel . *Proc. 20 th Int. Conf. on Water Jetting*, (20 th Int. Conf. on Water JettingGraz, Austria) 2010. October 20-22.